JOURNAL OF MATERIALS SCIENCE 31 (1996) 3081–3085

XPS study on composition and structure of epitaxial $KTa_{1-x}Nb_xO_3$ (KTN) thin films prepared by the sol–gel process

C. J. LU*§, A. X. KUANG§, G. Y. HUANG§, S. M. WANG§
*National Laboratory of Solid State Microstructure and Department of Physics, Nanjing University, Nanjing 210093, P. R. China and
§Department of Physics, Hubei University, Wuhan 430062, P. R. China

Epitaxial KTN (x = 0.35) thin films were prepared on (100) $SrTiO_3$ substrates by the sol–gel process. In this paper, wide and narrow scans of XPS analysis were studied on the surface of the KTN thin films before and after Ar^+ sputtering for 10 min. The results show that no impurity or residual carbon was observed in the films, except for some carbon contamination caused by handling and pumping oil on the surface of the films. The chemical composition of the films is in good agreement with the stoichiometry of the starting materials, as demonstrated by the ICP results. The valence states of the ions indicated that the films are KTN with a perovskite structure. XPS spectra of the films after Ar^+ sputtering differ considerably from those of the as-grown films, which may be attributable to the preferred sputtering of potassium and to new valence states produced during the Ar^+ bombardment. In addition, it was confirmed by the angle resolution XPS results that the chemical composition was well-distributed and that no other phase was observed apart from KTN in the near-surface region of the films.

1. Introduction

Potassium tantalate niobate ($KTa_{1-x}Nb_xO_3$ or KTN) has received a great deal of attention as a ferroelectric material possessing the perovskite structure [1]. Because of its piezoelectric, pyroelectric, and electro–optic properties, the crystal is of interest for application in band filters, infrared detectors, and electro–optic modulators [2–5]. The highest quadratic electro–optic coefficients are found in the nonferroelectric cubic phase of KTN at (x = 0.35) at room temperature [6]. Direct thin film preparation appears to be much more suitable for electro–optical as well as some other applications, since not only is the bulk-homogeneity problem circumvented, but also the cutting and polishing of thin slabs can be avoided. In addition these films also afford the possibility for use in silicon very-large-scale integration technologies. Therefore, the demand for KTN thin films for application in electro–optics has increased in recent years.

Recently, we successfully fabricated epitaxial KTN (x = 0.35) thin films on (100) $SrTiO_3$ substrates by the sol–gel process [7, 8]. In order to obtain high quality KTN thin films with desired properties by the sol–gel process, it is particularly important to determine the chemical composition and its depth profile in the films and also the valence states of ions in the films because potassium is very volatile and the films are directly deposited from organic solution. X-ray photoelectron spectroscopy (XPS) is an effective surface analysis technique, and it has been employed to determine the chemical composition and its depth profile in Pb-containing ferroelectric thin films [9–12]. The effect of the Ar^+ bombardment on the ferroelectric thin films was not reported. In this paper, we have analysed wide and narrow XPS scans of the epitaxial KTN thin films before and after Ar^+ sputtering for 10 min and also the angle resolution XPS (ARXPS) of the as-grown films. In addition we have studied the effect of the Ar^+ bombardment on the films. This work is important not only to explore the optimal conditions for KTN film preparation but also to improve the properties of the films by ion beam techniques.

2. Sample preparation and handling procedures

The film in our experiments was prepared on a (100) $SrTiO_3$ substrate by the spinning of the sol–gel solution. The preparation conditions were published elsewhere [7, 8]. The film was annealed at 700 °C for 2 h and its thickness was about 600 nm. The X-ray diffraction (XRD) pattern of the film is shown in Fig. 1; only the (100), (200), and (300) KTN peaks, in addition to the expected substrate reflections are found, which demonstrates the excellent orientation of the sample. The epitaxy of the KTN film was also proved by the reflection pattern high energy electron diffraction (RHEED) technique [7]. The period between the film preparation and the XPS measurements was within

0022–2461

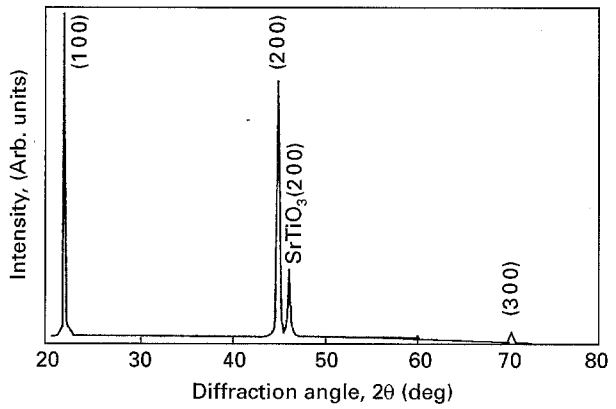

Figure 1 XRD pattern of the KTN thin film used in the experiment.

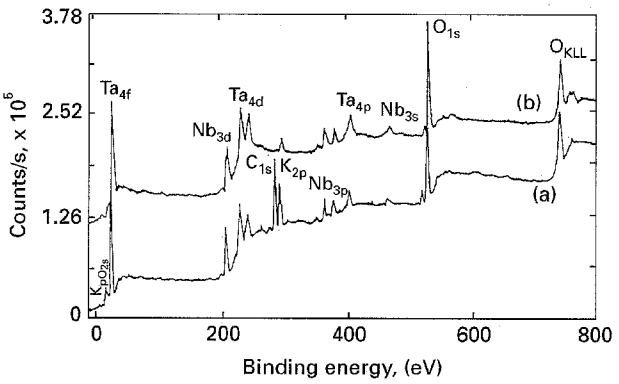

Figure 2 Wide-scan XPS spectra of the KTN thin film surface. (a) curve 1 is before the sputtering (b) is curve 2 after 10 min of Ar^+ sputtering.

two weeks, and the sample was stored in a clean dry ambient atmosphere at room temperature.

3. Results and discussion

3.1. XPS analysis for composition

It is a commonly asked question as to whether residual carbon caused by carbonization of the organic groups can be completely removed from the sol–gel derived films during later heat-treatment. To identify the composition of the films, XPS analyses were carried out by the Escalab-MKII spectrometer using Mg K_α (1253.6 eV) radiation. Fig. 2 gives the wide-scan XPS spectra of the KTN (x = 0.35) thin films before (curve 1) and after Ar^+ sputtering for 10 min (curve 2) in the binding energy range of 0–800 eV. All of the binding energies at various peaks were calibrated using the binding energy of C_{1s} (284.6 eV) as a standard. As is shown in Fig. 2, all the peaks can be ascribed to XPS peaks of the elements K, Ta, Nb, O, and C, as well as the O_{KLL} Auger peak. The C_{1s} peak disappeared after the surface of the specimen was bombarded by a 6 keV Ar^+ beam for 10 min. The results suggest that either no impurity or residual carbon exists in the films or that their atomic percentages are less than 0.1%. Carbon on the surface of the as-grown films is due to contamination caused by handling or pumping oil. On the other hand, Fig. 3 gives the narrow-scan XPS spectrum of the C_{1s} peak of the as-

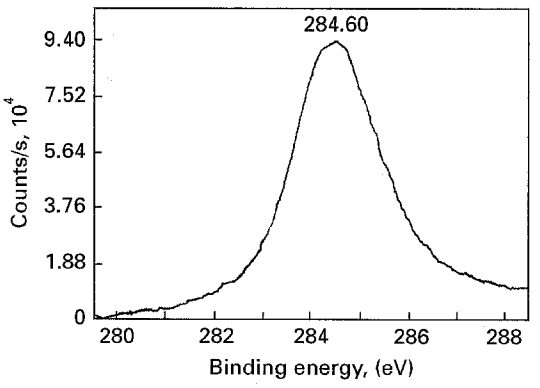

Figure 3 Narrow scan XPS spectrum of C_{1s} peak for the KTN thin film.

TABLE I Comparison of the chemical composition of KTN thin films derived from XPS spectra before and after Ar^+ sputtering for 10 min (stoichiometry) with the ICP results

	K_{2p}	Ta_{4f}	Nb_{3d}	O_{1s}
Before Ar^+ sputtering	1.00	0.70	0.34	3.21
After Ar^+ sputtering	0.25	0.70	0.35	2.02
ICP results	1.00	0.67	0.34	...

grown films; the C_{1s} peak at 284.6 eV is symmetric and narrow, further confirming that carbon on the surface of the as-grown films comes from contamination. If the atomic percentage of carbon caused by carbonization of organic groups was more than 0.1% on the surface of the films, a C_{1s} sign should appear at 282.0 eV.

It can also be seen from Fig. 2 that the intensity of the K_{2p} peak after the Ar^+ sputtering decreased appreciably compared with the wide-scan XPS spectrum of the as-grown films. The results of the quantitative atomic composition analyses from XPS spectra before and after Ar^+ sputtering are given in Table 1. As is shown in Table 1, the atomic ratio Ta:Nb on the surface of the films was nearly equal to that after Ar^+ sputtering, while the deviation between the ratio value and that of the starting materials may be a result of experimental error. It is worth mentioning that the atomic ratio K/(Ta + Nb) in the near surface region of the films is close to the stoichiometry of the starting materials. However, the ratio value decreases seriously after Ar^+ sputtering, which is attributable to the loss of K caused by the preferred sputtering of K, and thus it cannot indicate the real composition in the bulk of the film. The chemical composition for the same specimen was also determined by inductively coupled plasma (ICP) measurements, and the results (see Table 1) were in good agreement with the atomic ratio of the starting materials, confirming further the above suggestion. Actually, no important weight loss was encountered over the annealing range 670–900 °C [8]. These data indicate that there is no tangible loss of any constituent from the top film surface by evaporation. The chemical composition of the film can be highly controlled when the KTN films were prepared by the sol–gel method. The moderate hydrolysis of the K–Ta–Nb complex alkoxide results in the formation

of metalloxane polymers in which K, Ta and Nb are homogeneously and intimately mixed in addition to a lower reaction temperature.

Obviously, no K enrichment was observed on the film surface. This result is quite different from those reported in recent publications [9–11] where Pb enrichment was believed to be an intrinsic phenomenon for Pb-contained ferroelectric thin films. The difference may be due to the different experimental details, but more possibly it is caused by the point that the effect of Ar^+ bombardment was not taken into consideration in either the XPS or AES depth profile process [9–11].

3.2. XPS analyses for chemical states

XPS spectra give not only quantitative compositional data, but also information on the chemical states of ions, from which the compounds existing near the surface region can be identified. The narrow-scan XPS spectra of K_{2p}, Ta_{4f}, Nb_{3d}, and O_{1s} peaks of the films before and after Ar^+ sputtering are shown in Figs 4–7, respectively. The analysis results are listed in Table II.

The narrow-scan XPS spectra of K_{2p} (see Fig. 4a), Ta_{4f} (see Fig. 5a), and Nb_{3b} (see Fig. 6a) peaks of the as-grown films are doublets, whilst that of the O_{1s} peak is a singlet (see Fig. 7a). According to the peak shapes and the binding energies of $K_{2p_{3/2}}$, $Ta_{4f_{7/2}}$, $Nb_{3d_{5/2}}$, and O_{1s} peak (see Table II), as well as by comparison with data from the literature [13], it can be deduced that the elements K, Ta, Nb, and O near the film surface exists in the form of $K(Ta,Nb)O_3$, $KTaO_3$, $KNbO_3$, and $K(Ta,Nb)O_3$ respectively. Namely, the near surface region of the films is $K(Ta,Nb)O_3$ possessing the perovskite structure.

Although the intensity of the K_{2p} peak decreased seriously after Ar^+ sputtering (see Fig. 4), its peak shape and binding energy do not change on the whole, which indicates that residual K on the surface of the films after Ar^+ sputtering still exists in the form of $K(Ta,Nb)O_3$ in spite of the serious preferential sputtering of K. However, quite different from the situation of the K_{2p} peak, the Ta_{4f} peak after Ar^+ sputtering became much wider than before (see Fig. 5b). A quantitative peak fitting procedure for the Ta_{4f} spectrum shows that it is composed of at least two

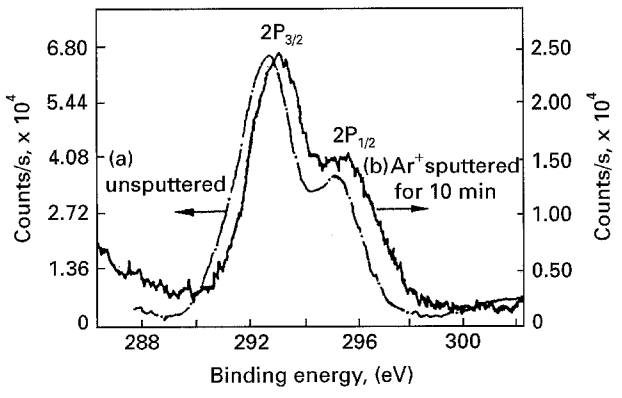

Figure 4 Narrow-scan XPS spectra of K_{2p} peak for the KTN thin film.

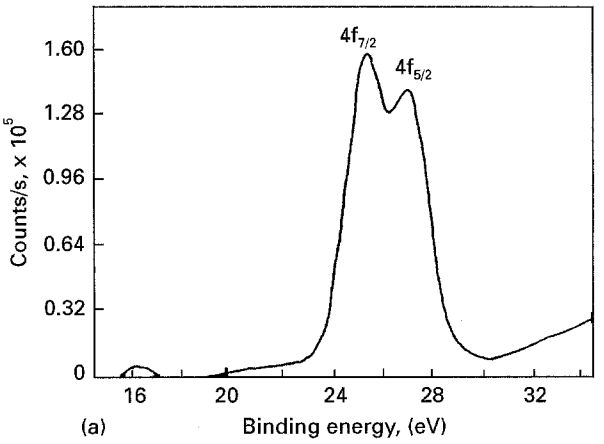

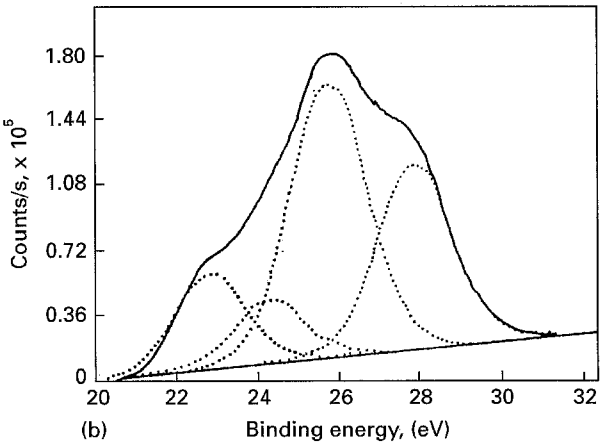

Figure 5 Narrow-scan XPS spectra of Ta_{4f} peak for the KTN thin film (a) before and (b) after Ar^+ sputtering.

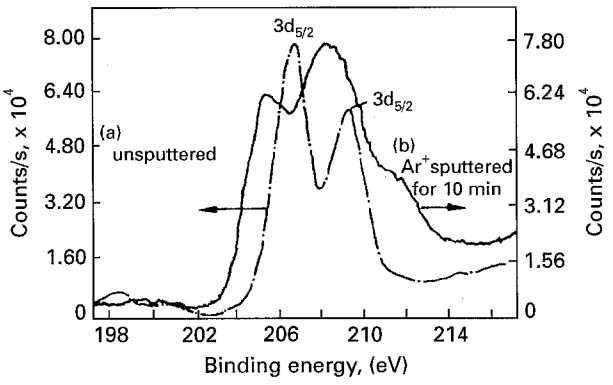

Figure 6 Narrow-scan XPS spectra of Nb_{3d} peak for the KTN thin film.

main doublets. The doublets could be ascribed to Ta and TaO_3^{-1} (see Table II), where the former is actually a Ta atom surrounded by oxides and so its binding energy is higher than that in pure tantalum. The narrow-scan XPS spectrum of the Nb_{3d} peak after Ar^+ sputtering (see Fig. 6b) is too complicated to decompose, but its deconvolution results show that it includes at least five main doublets (see Table II), which indicates that Nb near the surface of films after Ar^+ sputtering exists mainly in the form of NbO, NbO_2, and NbO_3^{-1} etc. Because the binding energies of O_{1s} in $K(Ta,Nb)O_3$, NbO, NbO_2, NbO_3^{-1}, and TaO_3^{-1} are almost a value, the O_{1s} peak of the films after Ar^+

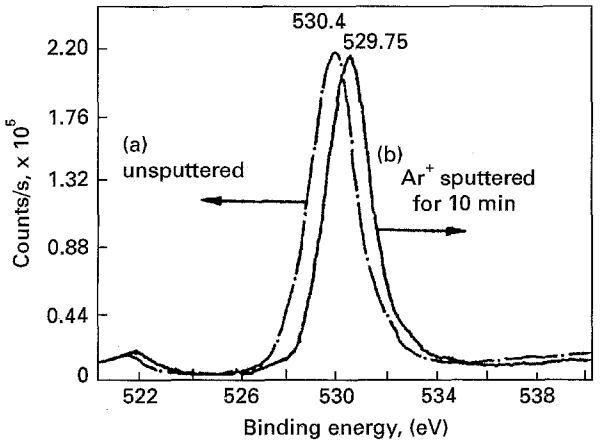

Figure 7 Narrow-scan XPS spectra of O_{1s} peak for the KTN thin film.

TABLE II The analysis results of narrow-scan XPS spectra for the KTN films

Sample	Narrow-scan spectrum	Binding energy (eV)	Chemical state [13]
Before Ar^+ sputtering	$K_{2p_{3/2}}$	292.70	$K(Ta,Nb)O_3$
	$Ta_{4f_{7/2}}$	25.40	$KTaO_3$
	$Nb_{3d_{5/2}}$	206.70	$KNbO_3$
	O_{1s}	530.40	$K(Ta,Nb)O_3$
	$K_{2p_{3/2}}$	293.00	$K(Ta,Nb)O_3$
	$Ta_{4f_{7/2}}$	22.85	Ta*
		25.80	TaO_3^{-1}
After Ar^+ sputtering	$Nb_{3d_{5/2}}$	203.15, 204.05	NbO
		204.85, 205.40	NbO_2
		206.50	NbO_3^{-1}
	O_{1s}	929.75	NbO, NbO_2, TaO_3^{-1}, NbO_3^{-1}, $K(Ta,Nb)O_3$

*Ta atoms surrounded by oxides.

sputtering is narrow and close to that of the as-grown films, as is shown in Fig. 7.

The narrow-scan XPS spectra of Ta_{4f} and Nb_{3d} of the films were markedly changed after Ar^+ sputtering. However, the results did not imply that there are serious differences between the valence states of ions near the surface and in the bulk of the films, since the XRD pattern (see Fig. 1) recorded for the same specimen showed that the film is KTN with a perfect perovskite structure. Actually, it is probably due to the production of many new dangling bonds created by the preferential sputtering of K during the Ar^+ bombardment. In general, preferential sputtering of an element is related to changes of valence states in a multi-constituent compound. It has often been observed that some ions with high oxidation states were reduced to lower oxidation states during the XPS depth profile process [12, 14–16], which is very similar to the effect of a heat-treatment in a vacuum. Therefore, the effect of the Ar^+ bombardment should be taken into consideration when ferroelectric thin films are prepared and processed by an ion beam technique, such as ion implantation and ion beam mixing.

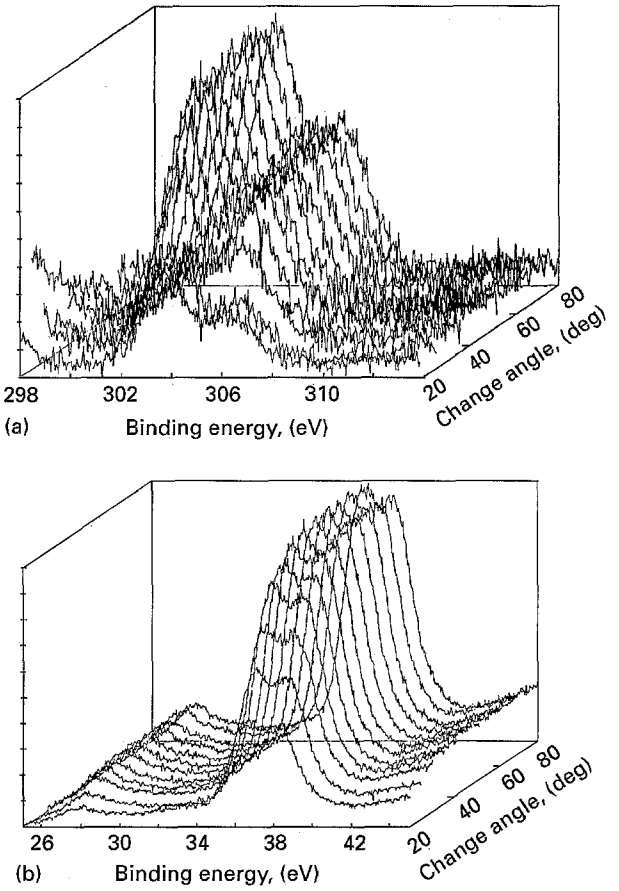

Figure 8 Narrow-scan ARXPS spectra of (a) K_{2p} and (b) Ta_{4f} peaks for the as-grown KTN thin film.

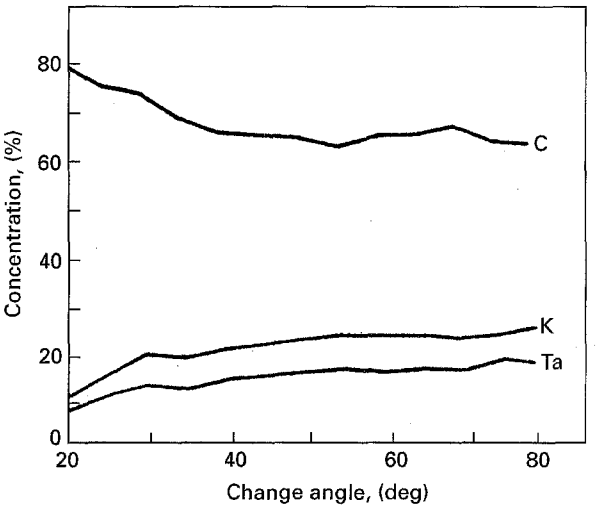

Figure 9 Depth analysis of the as-grown KTN film on the surface layer.

3.3. ARXPS analyses for depth profile

Seeing that Ar^+ sputtering was not applicable to KTN thin films, the ARXPS method was used to analyse the depth profile of the films. The step of the start off angle of the photoelectrons was 5° and the other experimental conditions were the same as those above. The narrow scan XPS spectra of K_{2p} and Ta_{4f} peaks at 20–80° for the as-grown films are displayed as two three-dimensional figures, in Fig. 8. Even though the intensities of the K_{2p} and the Ta_{4f} peaks are weak and different to each other at low angles as a result of angle effect and the serious carbon contamination on the surface, they

are relatively stable at high angles and moreover the shape of the peaks are identical over the whole measuring range. Fig. 9 gives the depth profile of the C, K and Ta elements on the surface layer of the films. Such an angular dependence of the analysis depth is often expressed as $D = 3\lambda \sin\theta$, where D, λ and θ are the analysis depth in the surface layer, the inelastic mean free pace (IMFP) and the starting angle of the photoelectron, respectively. In the experiment λ is about 1.2–2 nm, so the analysis depth of the film surface layer is in the range of 1.0–5.5 nm. It is thus clear from Figs 8 and 9 that the chemical states of K and Ta are identical and that the atomic ratio K : Ta is well-distributed in the depth range, supporting further conclusions in Sections 3.1 and 3.2.

4. Conclusion

The chemical composition, its depth profile and chemical bonding analyses were performed by using XPS, ARXPS, and ICP measurements for epitaxial KTN($x = 0.35$) thin films deposited by a sol–gel process. It was found that the chemical composition of the films is in good agreement with the stoichiometry of the starting materials and that it is well-distributed in the whole depth range. No impurity or residual carbon was observed in the films, except for some carbon contamination, caused by handling and pumping oil, on the surface of the films. The K, Ta, Nb and O atoms exist mainly in the form of $K(Ta,Nb)O_3$ in both the near surface and bulk regions. After Ar^+ sputtering the XPS spectra of the films differ markedly from those before, which is attributed to preferential sputtering of K and to new valence states of ions produced during the Ar^+ bombardment. The effect of the Ar^+ bombardment should be taken into consideration when KTN thin films are prepared or processed by low energy ion beam techniques.

Acknowledgements

The first author would like to thank Professor D. F. Wang for the XPS measurements and helpful discussion. This work was supported by the Chinese National 863 Advanced Technology Project (715-03-02-01B).

References

1. S. TRIEOWASSER, *Phys. Rev.* **114** (1959) 63.
2. J. E. GEUSIC, S. K. KURTS, L. G. VAN UITERT and S. H. WEMPLE, *Appl. Phys. Lett.* **4** (1964) 141.
3. F. S. CHEN, J. E. GEUSIC, S. K. KURTS, L. G. VAN UITERT and S. H. WEMPLE, *J. Appl. Phys.* **37** (1966) 388.
4. O. M. STAFUDD and M. Y. PINES, *J. Opt. Soc. Amer.* **62** (1972) 1153.
5. A. J. FOX, *Appl. Opt.* **14** (1975) 343.
6. R. ORLOWSKI, L. A. BOATNER and E. KRATIG, *Opt. Commun.* **35** (1980) 45.
7. D. H. BAO, A. X. HUANG and S. M. WANG, *Chin. Sci. Bull.* **37** (1992) 1470 (in Chinese).
8. A. X. KUANG, C. J. LU and G. Y. HUANG, *J. Crystal Growth* **149** (1995) 80.
9. Z. H. QIAN, D. Q. XIAO, J. G. ZHU and Z. S. LI, *J. Appl. Phys.* **74** (1993) 224.
10. S. G. YOON, J. D. PARK, J. H. CHOI and H. G. KIM, *J. Vac. Sci. Tech.* **A9** (1991) 281.
11. S. IBUKI, T. NAKAYAWA, M. OKUYAMA and Y. HANAKAWA, *Jpn. J. Appl. Phys.* **29** (1990) 532
12. C. J. LU, A. X. KUANG, G. Y. HUANG and S. M. WANG, *J. Appl. Phys.* (in press).
13. C. D. WAGNER, W. M. RIGGS, L. E. DAVIS, J. F. MOULDER and G. E. MUILENBERG, "Handbook of X-ray Photoelectron Spectroscopy" (Perkin-Elmer Corporation Physical Electronics Division, U.S.A., 1979).
14. S. H. LIU, D. H. WANG and C. H. PAN, X-ray Photoelectron Spectroscopy Analysis (in Chinese) (Science Press, Beijing, 1988) p. 250.
15. S. HOFMAN and J. M. SANZ FRESENIUS, *Z. Anal. Chem.* **314** (1983) 215.
16. X. Q. FONG, Z. X. REN and C. LI, *Acta Phys.* **33** (1984) 231 (in Chinese).

Received 10 August
and accepted 21 December 1995